# Coupled Dynamics of Photosynthesis, Transpiration, and Soil Water Balance. Part I: Upscaling from Hourly to Daily Level

EDOARDO DALY

*Dipartimento di Idraulica Trasporti e Infrastrutture Civili, Politecnico di Torino, Turin, Italy, and Department of Civil and Environmental Engineering and Princeton Environmental Institute, Princeton University, Princeton, New Jersey*

AMILCARE PORPORATO

*Department of Civil and Environmental Engineering, Duke University, Durham, North Carolina*

IGNACIO RODRIGUEZ-ITURBE

*Department of Civil and Environmental Engineering and Princeton Environmental Institute, Princeton University, Princeton, New Jersey*

(Manuscript received 20 May 2003, in final form 16 December 2003)

ABSTRACT

The governing equations of soil moisture dynamics, photosynthesis, and transpiration are reviewed and coupled to study the dependence of plant carbon assimilation on soil moisture. The model follows the scheme of the soil–plant–atmosphere continuum (SPAC) and uses a simplified model of the atmospheric boundary layer to arrive at an upscaled, parsimonious representation at the daily time scale. The analysis of soil moisture, transpiration, and carbon assimilation dynamics provides an assessment of the role of soil, plant, and boundary layer characteristics on the diurnal courses of photosynthesis and transpiration rates, while the subsequent upscaling at the daily level provides a functional dependence of stomatal conductance on soil moisture that is in good agreement with field experiments. The upscaled dependence of transpiration and carbon assimilation on soil moisture is used in Part II of this paper to explore the impact of soil moisture dynamics on plant conditions when rainfall variability is explicitly considered.

## 1. Introduction

In water-limited ecosystems, soil moisture is the key variable controlling the transpiration and photosynthesis rates, the insurgence of plant water stress, the dynamics of vegetation growth and reproduction, as well as the long-term evolution of the ecosystems and the plant strategies of adaptation to climate change (e.g., Noy-Meir 1973; Stephenson 1990; Porporato and Rodriguez-Iturbe 2002; Knapp et al. 2002; and references therein). From the meteorological point of view, the land–atmosphere interaction crucially depends on soil moisture availability and plant transpiration, which control the water and heat fluxes between soil and the atmosphere (e.g., Dickinson et al. 1986; Sellers et al. 1986; Bonan 1995; Brubaker and Entekhabi 1995; Pollard and Thompson 1995; Foley et al. 1996; Sellers et al. 1997; Elthair 1998; Porporato et al. 2000). The dynamics of the soil–plant–atmosphere system also has deep implications for the evolution of carbon and nitrogen cycles in soils (e.g., Dickinson et al. 2002; Porporato et al. 2003; D'Odorico et al. 2003; and references therein), as soil moisture drives the decomposition of soil organic matter and controls the leaching and plant uptake of mineral nitrogen.

The soil–plant–atmosphere system hosts an intricate interconnection of processes that, at the same time, control and are controlled by the other components of the system. A striking example is vegetation that is both responsible for the soil water losses and suffers from water stress at low soil moisture levels. In this manner, the hydrologic cycle is closely connected to the plant physiological processes. As a consequence, any modeling effort has the additional difficulty of dealing with biological components for which the approach is still partly empirical. Moreover, the processes in the soil–plant–atmosphere system involve different time scales (e.g., from the hourly dynamics of stomatal control and transpiration to the soil moisture depletion at the daily time scale and the seasonal dynamics of plant growth) with components that are highly intermittent and unpredictable (rainfall in particular). The temporal upscaling of such processes is thus essential to understand

*Corresponding author address:* Dr. Amilcare Porporato, Dept. of Civil and Environmental Engineering, 127 Hudson Hall, Duke University, Durham, NC 27708.
E-mail: amilcare@duke.edu

© 2004 American Meteorological Society

which of the processes acting at the short time scales actually controls the long-term dynamics of the water and carbon fluxes and the related evolution of ecosystems.

The goal of the present investigation is to link the temporal evolution of soil moisture, transpiration, and photosynthesis to the diurnal evolution of the atmospheric boundary layer and then integrate the results at the daily and growing season time scales. In this paper, we begin at the hourly time scale by reviewing and suitably coupling simple and parsimonious models of the soil–plant–atmosphere continuum (SPAC) and photosynthesis (e.g., Jarvis 1976; Farquhar et al. 1980; McNaughton and Spriggs 1986; Leuning 1995; Sperry et al. 1998; Lhomme 2001; Katul et al. 2003) to derive the functional dependence of transpiration and carbon assimilation on soil moisture at the daily level. Particular attention is devoted to obtaining a physical interpretation of the role of soil and vegetation parameters in the upscaled temporal dynamics of the SPAC and to elucidating the physical bases of the empirical representation of the processes commonly used to model the soil moisture dynamics at the daily time scale (e.g., Federer 1979; Cordoba and Bras 1981; Dingman 1994; Rodriguez-Iturbe et al. 1999; Laio et al. 2001). In a companion paper (Daly et al. 2004, hereafter Part II), the results are successively incorporated into a stochastic model for soil moisture evolution to analyze the probabilistic structure of plant carbon assimilation under fluctuating climatic conditions during a growing season.

Despite the simplification that will be used (e.g., simple scaling from leaf-level to stand-level conductance, constant wind and atmospheric stability, absence of cloud cover, homogeneous vegetation, and soil moisture conditions), the resulting model reliably reproduces the basic links among stomatal conductance, photosynthesis, transpiration, and soil water balance, and thus fulfills our goal of obtaining a physical interpretation of the daily time scale from an understanding of the basic processes acting at the hourly level. The model, however, is not intended to predict the precise diurnal behavior or to quantitatively estimate the parameters of the functional dependence of transpiration and assimilation on soil moisture at the daily time scale. Therefore, after the typical form of these links and their physical origin have been clarified, the relevant parameters need to be estimated directly from measured data (as in Rodriguez-Iturbe et al. 1999; Laio et al. 2001; Porporato et al. 2001). On the other hand, when the interest is in more quantitative predictions at the hourly level, a more detailed discussion of the scaling of the soil–plant–atmosphere continuum to the stand level (e.g., Jarvis and McNaughton 1986; Leuning et al. 1995) as well as a critical comparison of the results of more complete models of integrated dynamics of water balance, ecophysiology, and meteorology (e.g., Bonan 1995; Dickinson et al. 1986; Pollard and Thompson 1995; Sellers et al. 1986, 1997; Williams et al. 1996; Baldocchi and Meyers 1998; Siqueira et al. 2002) is necessary.

The paper is organized as follows. After the development of the equations for the water movement through the SPAC, the modeling of the various conductances is presented. Two stomatal functions are considered according to the approaches of Jarvis (1976) and Leuning (1990, 1995), and their relation to photosynthesis and carbon assimilation is discussed with reference to the classical model of Farquhar et al. (1980) for the photosynthesis of $C_3$ plants. The results of the numerical integration at the hourly time scale are then presented, and the diurnal patterns of transpiration, assimilation, and leaf stomatal conductance are analyzed as soil moisture decays from well-watered to advanced-drought conditions. The functional dependence of leaf stomatal conductance is integrated at the daily level and found to favorably compare with measured data from the literature. Part II carries on the investigation of the upscaled dynamics at the daily time scale with the inclusion of the stochastic component in the soil moisture dynamics.

## 2. Transpiration and soil water balance at the hourly time scale

According to the framework of the SPAC, the water is taken up by the roots, flows through the xylem, and exits through the leaf stomata to the atmosphere, following a path of decreasing water potential, from the soil at $\psi_s$, through the leaves at $\psi_l$, to the atmosphere at $\psi_a$. Typically, the water flow inside the plant is assumed to take place as a succession of steady states (i.e., considering the system adjustment to the time-varying equilibrium conditions as practically instantaneous). For the sake of simplicity we assume vertically averaged soil moisture dynamics [see Guswa et al. (2002) for a critical discussion of the vertical spatial upscaling of the soil water balance] as well as uniform canopy coverage by vegetation. The exchanges between vegetation and atmosphere are modeled using the standard single big-leaf schematization.

Under these assumptions, the appropriate equation for soil moisture dynamics at the hourly time scale during interstorm periods may be written as

$$nZ_r\frac{ds}{dt} = -E - \mathrm{EV} - L, \tag{1}$$

where $s$ is the relative soil moisture averaged over the root depth $Z_r$; $n$ is porosity; and $E$, EV, and $L$ are the transpiration, evaporation from the soil, and the leakage, respectively, expressed in terms of unit ground area. As EV is typically a small fraction of transpiration for well-vegetated ecosystems (e.g., Scholes and Walker 1993), its precise modeling is not crucial. Here, for reasons of mathematical convenience in the future stochastic analysis, EV is simply assumed to be equal to $\mathrm{EV}_{\max}$ for $s$ higher than the so-called wilting point, $s_w$, and to decrease linearly to zero at the hygroscopic point, $s_h$. Leak-

TABLE 1. Parameter values used in the model.

| Parameter | Value | Units | Description |
|---|---|---|---|
| $a$ | 8 | | Parameter accounting for root growth |
| $a_1$ | 18 | | Eq. (9) |
| $c$ | 2 | | Parameter of the vulnerability curve |
| $c_a$ | 350 | $\mu$mol mol$^{-1}$ | Atmospheric carbon concentration |
| $c_p$ | 1012 | J kg$^{-1}$ K$^{-1}$ | Specific heat of air |
| $d$ | 2 | MPa | Parameter of the vulnerability curve |
| $D_{xJ}$ | 1250 | Pa | Eq. (8) |
| $D_{xL}$ | 300 | Pa | Eq. (9) |
| $\mathrm{EV}_{\max}$ | 0.2 | mm d$^{-1}$ | Eq. (1) |
| $g_{p\max}$ | 11.7 | $\mu$m MPa$^{-1}$ s$^{-1}$ | Maximum plant conductance |
| $g_a$ | 20 | mm s$^{-1}$ | Atmospheric conductance (unit ground area) |
| $g_b$ | 20 | mm s$^{-1}$ | Leaf boundary layer conductance (unit leaf area) |
| $g_{s\max}$ | 25 | mm s$^{-1}$ | Maximum stomatal conductance (unit leaf area) |
| $h_0$ | 50 | m | Boundary layer height at night |
| $k_1$ | 0.005 | m$^2$ W$^{-1}$ | Eq. (6) |
| $k_2$ | 0.0016 | K$^{-2}$ | Eq. (6) |
| $p_a$ | $1.013 \cdot 10^5$ | Pa | Air pressure |
| $T_{\mathrm{opt}}$ | 298 | K | Eq. (6) |
| $\lambda_w$ | $2.5 \cdot 10^6$ | J kg$^{-1}$ | Latent heat of water vaporization |
| $\rho$ | 1.2 | kg m$^{-3}$ | Air density |
| $\phi_{\max}$ | 500 | W m$^{-2}$ | Maximum available energy |
| $\psi_{l1}$ | $-0.05$ | MPa | Eq. (7) |
| $\psi_{l0}$ | $-4.5$ | MPa | Eq. (7) |
| $\psi_{l_{A1}}$ | $-0.5$ | MPa | Eq. (13) |
| $\psi_{l_{A0}}$ | $-4.5$ | MPa | Eq. (13) |

age losses are assumed to follow the behavior of the hydraulic conductivity (e.g., Clapp and Hornberger 1978), $L = K = K_s s^{2b+3}$, where $K_s$ is the saturated hydraulic conductivity and $b$ is the exponent of the retention curve,

$$\psi_s = \overline{\psi}_s s^{-b}, \tag{2}$$

where $\overline{\psi_s}$ is the soil water potential at saturation (e.g., Clapp and Hornberger 1978). In the absence of rain, the solution of Eq. (1) represents the decay of soil moisture starting from a given initial condition and provides the boundary condition to the SPAC in terms of water potential.

The flux of water per unit ground area from the roots to the leaves is modeled as proportional to the water potential gradient (van den Honert 1948) as

$$E = g_{srp}(\psi_s - \psi_l), \tag{3}$$

where $g_{srp}$ is the soil–root–plant conductance per unit ground area, $g_{srp} = (L_{\mathrm{AI}} g_{sr} g_p)(g_{sr} + L_{\mathrm{AI}} g_p)^{-1}$, that is, the series of the soil–root conductance per unit ground area, $g_{sr}$, and plant conductance in terms of unit leaf area, $g_p$. Soil–root–plant conductance depends on both leaf area index ($L_{\mathrm{AI}}$; i.e., the leaf area per unit ground area) and root area index ($R_{\mathrm{AI}}$; i.e., the root area per unit ground area), which modulate the relative importance of root and xylem conductance, determining which part contributes more to the limitation of water flow (e.g., Sperry et al. 1998, 2002).

TABLE 2. Soil parameters used in the model.

| | $\overline{\psi}_s$ (MPa) | b | $K_s$ (cm day$^{-1}$) | n | $s_h$ |
|---|---|---|---|---|---|
| Loamy sand | $-0.17 \cdot 10^{-3}$ | 4.38 | 100 | 0.42 | 0.08 |
| Loam | $-1.43 \cdot 10^{-3}$ | 5.39 | 20 | 0.45 | 0.19 |

The soil–root conductance is assumed to be proportional to the soil hydraulic conductivity divided by the average distance, $L_{sr}$, traveled by water from the soil to the root surface. A simplified cylindrical root model allows us to link $L_{sr}$ to the root depth and the root area index (Katul et al. 2003),

$$g_{sr} = \frac{K\sqrt{R_{\mathrm{AI}}}}{\pi g \rho_w Z_r}, \tag{4}$$

where $g$ is the gravitational acceleration, and $\rho_w$ is the density of water. Considering that roots respond continuously to soil moisture dynamics, the plant water availability (and thus soil–root conductance) cannot be judged solely on the basis of soil parameters (Larcher 1995, p. 229). It is therefore reasonable to assume that the decrease of $g_{sr}$ due to $K$ as soil dries is in part compensated by the plant through root growth so that, for moderate soil water deficit, the distance $L_{sr}$ reduces when soil water availability decays (e.g., Larcher 1995). This is simply modeled by correcting $R_{\mathrm{AI}}$ with a multiplicative term that attenuates the reduction due to $K$, that is, $R_{\mathrm{AI}} = R^*_{\mathrm{AI}} \times s^{-a}$, where $R^*_{\mathrm{AI}}$ is the root area index in well-watered conditions, and $a$ is a parameter that varies from species to species. The parameters used in the simulations, reported in Tables 1 and 2, are chosen to reproduce typical values of $g_{sr}$ found in the literature (e.g., Nobel 1999).

Plant conductance, $g_p$, drops when the water potential

is too low because of xylem cavitation; this decay is modeled by a vulnerability curve (e.g., Sperry et al. 1998; Katul et al. 2003), $g_p = g_{p\max} \exp[-(-\psi_l/d)^c]$, where $d$ and $c$ are such that $g_p$ is equal to $g_{p\max}$ for high values of $\psi_l$ and close to 0 for low $\psi_l$ (see Table 1).

Under steady-state conditions and neglecting cuticular transpiration, the flux inside the plant must equal the transpiration rate, which is assumed to be proportional to the specific humidity gradient between inside the leaves and the atmosphere. The Penman–Monteith combination approach avoids the explicit dependence of transpiration on $T_l$, leading to

$$E = \frac{(\lambda_w \gamma_w g_{\rm ba} \rho D + S\phi) g_s L_{\rm AI}}{\rho_w \lambda_w [\gamma_w (g_{\rm ba} + g_s L_{\rm AI}) + g_s L_{\rm AI} S]}, \quad (5)$$

where $\lambda_w$ is the latent heat of water vaporization, $\gamma_w = (p_a c_p)/(0.622\lambda_w)$ is the psychrometric constant, $D$ is the potential saturation deficit of the air [i.e., the difference between the air relative humidity at saturation and $q(T_a)$], $S$ is the slope of curve relating saturation vapor pressure to temperature, $\phi$ is the leaf available energy (see appendix A), $g_s$ is the stomatal conductance (per unit leaf area), and $g_{\rm ba}$ (per unit ground area) is the series between the conductance of the leaf boundary layer $g_b$ (per unit leaf area) and of the atmospheric boundary layer $g_a$ (per unit ground area), both assumed for simplicity to be constant.

In summary, the system of equations (1), (2), (3), and (5) in the unknowns $s$, $E$, $\psi_s$, and $\psi_l$ is determined once $g_s$ and the time course of the meteorological variables (e.g., radiation, air specific humidity, and potential temperature during the day) are given or modeled. The latter ones are computed by solving a simple model for the boundary layer dynamics (see appendix A), while the modeling of $g_s$ is now discussed in detail.

## 3. Stomatal function

Plants control the opening of the stomata to regulate the water and $CO_2$ transit during transpiration and photosynthesis. This allows them to maintain turgor and reduce dehydration as well as to control leaf temperature and maximize carbon assimilation. The complex mechanisms of stomatal movement depend on both plant physiology and environmental factors. No complete model for their functioning has been developed so far, so that empirical approaches are usually employed. In what follows two well-known models for the stomatal functions are discussed and compared. Although apparently very different, we anticipate here that the two models give qualitatively similar results, especially when upscaled to the daily level, thus providing confidence on the validity of the functional dependence of transpiration and assimilation that will be obtained (Part II).

### a. Jarvis's formulation

Jarvis's empirical formulation (Jarvis 1976; Jones 1992; Lhomme et al. 1998; Lhomme 2001) uses a multiplicative relationship of functions of the main factors affecting stomatal movement, such as solar radiation, ambient temperature, leaf water potential, potential saturation deficit, and $CO_2$ concentration, as

$$g_s = g_{\rm smax} f_\phi(\phi) f_{T_a}(T_a) f_{\psi_l}(\psi_l) f_D(D) f_{\rm CO_2}({\rm CO_2}), \quad (6)$$

where $g_{\rm smax}$ is the maximum stomatal conductance when none of the factors is limiting. The functions in Eq. (6) are obtained from controlled environment studies and account separately for the influence of each variable (Fig. 1). A brief discussion of these functions is useful to understand the links of Jarvis's formulation with the more physiological approach described in the next subsection.

The direct effect of increasing light is usually expressed as an exponential function $f_\phi(\phi) = 1 - \exp[-k_1\phi]$ (Fig. 1a), where $k_1$ is equal to 0.005 $m^2\ W^{-1}$ (Jones 1992, p. 156). For simplicity, $\phi$ is assumed to be equal to the leaf available energy. In general, stomata open as ambient temperature increases up to an optimum value, $T_{\rm opt}$, after which they start closing (Fig. 1b). A simple function commonly used is $f_{T_a} = 1 - k_2(T_a - T_{\rm opt})^2$, with $k_2 = 0.0016\ K^{-2}$ and $T_{\rm opt} = 298$ K (Lhomme et al. 1998).

Regarding leaf water potential, it is assumed (see Jones 1992; Lhomme et al. 1998; Lhomme 2001) that in well-watered conditions there is no control of $\psi_l$ up a certain point $\psi_{l_1}$, from which stomatal conductance starts decreasing to zero when $\psi_l$ drops to $\psi_{l_0}$ (Fig. 1c), that is,

$$f_{\psi_l}(\psi_l) = \begin{cases} 0 & \text{for } \psi_l < \psi_{l_0} \\ \dfrac{\psi_l - \psi_{l_0}}{\psi_{l_1} - \psi_{l_0}} & \text{for } \psi_{l_0} \le \psi_l \le \psi_{l_1} \\ 1 & \text{for } \psi_l > \psi_{l_1}. \end{cases} \quad (7)$$

The parameters $\psi_{l_1}$ and $\psi_{l_0}$ are taken here equal to $-0.05$ and $-4.5$ MPa, respectively, in agreement with measured values of $C_3$ plants in semiarid ecosystems (Scholes and Walker 1993; Bonan 2002).

Since in many species an increase in water vapor deficit reduces stomatal conductance independently of $\psi_l$, a function $f_D(D)$ describing a direct stomatal sensitivity to $D$ is also often adopted. Following Leuning (1995) (see also Lohammer et al. 1980), we assume the relation

$$f_D(D) = \frac{1}{1 + D/D_x}, \quad (8)$$

where $D_x$ is 1250 Pa (e.g., Leuning 1995).

Finally, stomata are sensitive to the atmospheric $CO_2$ concentration $c_a$, because when $c_a$ decreases they open to maximize photosynthesis. However, as the $CO_2$ concentration is almost constant during the day, $f_{\rm CO_2}({\rm CO_2})$

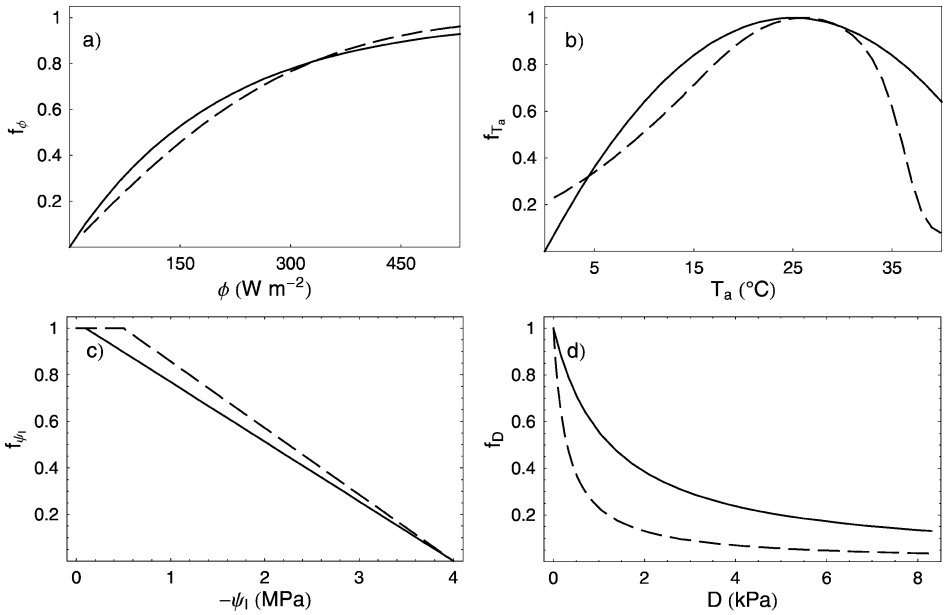


FIG. 1. Functions controlling stomatal response to the environment: (a) solar irradiance, (b) leaf temperature, (c) leaf water potential, and (d) water vapor deficit following Jarvis's (continuous line) and Leuning's (dashed line) approaches.

is seldom included in Eq. (6) (Lhomme 2001). As will be seen, this is important in the comparison with Leuning's approach.

### *b. Leuning's physiological formulation*

The model introduced by Ball et al. (1987) and improved by Leuning (1990, 1995) is based on the observed linear dependence of $CO_2$ stomatal conductance, $g_{s,CO_2}$, on net assimilation rate for normal environmental conditions. Leuning's formulation is

$$g_{s,CO_2} = a_1 A_n \frac{f_D(D)}{c_s - \Gamma^*}, \tag{9}$$

where $A_n$ is the net carbon assimilation per unit leaf area, $a_1$ is an empirical constant, whose typical value is around 15 (Leuning 1995), $\Gamma^*$ is the $CO_2$ compensation point (see appendix B), and $c_s$ is the carbon concentration at the leaf surface [the latter is related to the $CO_2$ atmospheric concentration; see Fig. 2 and Eq. (10)]. The same Eq. (8) is used in Eq. (9) for $f_D(D)$, but with $D_x = 300$ Pa (Leuning 1995) to match the maximum transpiration and assimilation rates of Jarvis's approach. For the same reason, we do not use saturation deficit at the leaf surface as in the original Leuning model. The residual (i.e., cuticular) value of conductance is assumed to be negligible in Eq. (9).

Different from Jarvis's approach, which completely determines $g_s$, Eq. (9) requires a model for the net carbon assimilation $A_n$ and thus for leaf photosynthesis and respiration. Such a model, which is described in the next section, also suggests some interesting connections with Jarvis's formulation.

## 4. Leaf carbon assimilation and photosynthesis

Photosynthesis is the process, occurring in the chloroplasts of the leaves, by which light energy is absorbed by green plants and used to produce carbohydrates from carbon dioxide and water. We schematically review its basic functioning while we define both notation and terminology.

1) *Light reactions.* Light energy is first absorbed by pigment molecules (mostly chlorophyll) and transferred to reaction centers where a series of biochemical reactions is initiated to create reducing power in the form of reduced nicotinamide adenine dinucleotine phosphate (NADPH) and chemical energy in the form of adenosine triphosphate (ATP). Water is necessary in this phase as it is oxidized into two protons, two electrons, and 1/2 oxygen (photolysis). For this reason, leaf cells need to be well hydrated and the leaf water potential $\psi_l$ must be high, otherwise photosynthesis is reduced. This is important in water-controlled ecosystems (e.g., Larcher 1995; Bonan 2002) but is often neglected in the models. The water abundance in the leaf cells under unstressed conditions is the cause for the great amount of water lost by evaporation when the stomata are opened to allow $CO_2$ influx.
2) *Dark reactions.* NADPH and ATP are used to convert the $CO_2$ (taken up from the atmosphere through the stomata) into carbohydrates through the Calvin cycle. This consists of three phases:

   - *Carboxylation.* The five-carbon sugar ribulose-1,5-biphosphate (RuBP) combines with $CO_2$ and water

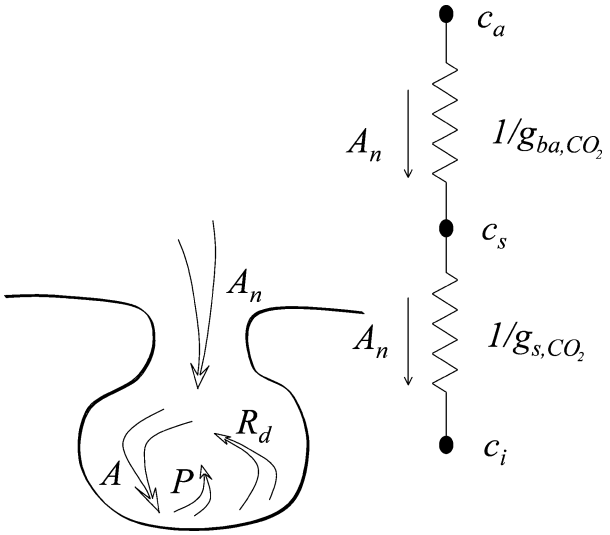


FIG. 2. Scheme of the gas balance within stomata.

to form three-carbon compounds ($C_3$ plants). This reaction is catalyzed by the rubisco enzyme (ribulose biphosphate carboxylase-oxygenase). The rate at which $CO_2$ is fixed by carboxylation will be indicated as $A$ (Fig. 2).

- *Reduction.* Next, the three-carbon compounds are modified using ATP and NADPH and then are in part transformed into carbohydrates.
- *Regeneration.* The remaining part of the modified three-carbon compounds is combined with additional ATP to regenerate RuBP.

During the Calvin cycle, rubisco also catalyzes the oxidation of RuBP, consuming oxygen and producing $CO_2$, in a process called *photorespiration* or *RuBP oxygenation*, which thus reduces by 30%–50% the net $CO_2$ uptake. The rate of photorespiration is indicated by $P$ (Fig. 2).

The opposite of photosynthesis is respiration, by which organic compounds are oxidized to produce energy to maintain plant functions and grow new tissues. Respiration takes place day and night in almost all the plant parts; in the leaf cells at daytime it occurs simultaneously during photosynthesis through the stomata. This type of respiration is called *dark respiration* or *daytime respiration* (e.g., Farquhar et al. 1980; Campbell and Norman 1998) and is distinct from photorespiration. The rate of daytime respiration is indicated by $R_d$ (Fig. 2).

### *Modeling net assimilation*

During the day, as a result of photosynthesis and respiration (and simultaneously with transpiration), plants exchange $CO_2$ with the environment as a diffusion process through the stomata. Under steady-state conditions, the net $CO_2$ flux per unit leaf area (i.e., net assimilation) is

$$A_n = g_{\mathrm{sba},CO_2}(c_a - c_i), \tag{10}$$

where $c_a$ and $c_i$ are the $CO_2$ concentrations in the atmosphere and leaf pores, respectively (Fig. 2), and $g_{\mathrm{sba},CO_2}$ is given by the series of the $CO_2$ stomatal, leaf boundary layer, and atmospheric conductance. It is usually assumed that $g_s = 1.6g_{s,CO_2}$ (e.g., Jones 1992), where the conductances are expressed in $\mathrm{mol}_{H_2O}\ \mathrm{m}^{-2}\ \mathrm{s}^{-1}$ and $\mathrm{mol}_{CO_2}\ \mathrm{m}^{-2}\ \mathrm{s}^{-1}$; the leaf boundary layer conductance $g_{b,CO_2}$ (per unit leaf area) is equal to $g_b/1.37$ (e.g., Bonan 2002), and the atmospheric conductance $g_{a,CO_2}$ (per unit ground area) is equal to $g_a$ (Jones 1992), where the conductances are expressed in $\mathrm{mol}_{H_2O}\ \mathrm{m}^{-2}\ \mathrm{s}^{-1}$ and $\mathrm{mol}_{CO_2}\ \mathrm{m}^{-2}\ \mathrm{s}^{-1}$, respectively.

As the adaptation of $CO_2$ concentration is much faster than the time scale of stomatal adjustment, the $CO_2$ balance inside the stomatal pores may be described by the steady-state condition (Fig. 2)

$$A_n = A - P - R_d. \tag{11}$$

The daytime respiration, $R_d$, depends on leaf temperature and is reduced at low leaf water potentials (e.g., Larcher 1995, p. 114). However, since $R_d$ is typically a small fraction of assimilation, it will be neglected for the sake of simplicity, as was also done by Dewar (1995) and Katul et al. (2003).

The rate of $CO_2$ fixation by carboxylation, $A$, and the rate of photorespiration, $P$, primarily depend on $\phi$, $c_i$, $T_l$, and $\psi_l$ (nutrient status and internal oxygen concentration are factors of secondary importance that are not considered here). As already mentioned, the limitation of $A$ and $P$ by low leaf water potential is seldom considered in modeling studies. However, such a dependence is crucial for studies, such as the present one, focusing on water-stressed conditions. For this reason, we assume an independent linear reduction of assimilation from an unrestricted rate at $\psi_{l_{A1}}$ to zero at $\psi_{l_{A0}}$, that is,

$$A_n \simeq A - P = A_{\psi_l} \times A_{\phi,c_i,T_l}(\phi, c_i, T_l), \tag{12}$$

where

$$A_{\psi_l} = \begin{cases} 0 & \text{for } \psi_l < \psi_{l_{A0}} \\ \dfrac{\psi_l - \psi_{l_{A0}}}{\psi_{l_{A1}} - \psi_{l_{A0}}} & \text{for } \psi_{l_{A0}} \le \psi_l \le \psi_{l_{A1}} \\ 1 & \text{for } \psi_l > \psi_{l_{A1}}. \end{cases} \tag{13}$$

Such a behavior is similar to those reported by Larcher (1995, 113–121), Tezara et al. (1999), and Bonan (2002, p. 303) and gives a dependence of $g_s$ on $\psi_l$ very similar to that used for Jarvis's model. Since the assimilation reduction caused by chemical action presumably starts for leaf water potential level lower than that corresponding to incipient stomata closure (Larcher 1995), $\psi_{l_1}$, $\psi_{l_{A1}}$ is assumed to be equal to $-0.5$ MPa. For simplicity, $\psi_{l_{A0}}$ is chosen equal to $\psi_{l_0}$ [Eq. (7)] since assimilation does not occur when stomata are completely closed.

The dependence of $(A - P)$ on $\phi$, $c_i$, and $T_l$ is given

TABLE 3. Parameters for the model of $C_3$ photosynthesis.

| Parameter | Value | Units | Description |
|---|---|---|---|
| $H_{Kc}$ | 59 430 | J mol$^{-1}$ | Activation energy for $K_c$ |
| $H_{Ko}$ | 36 000 | J mol$^{-1}$ | Activation energy for $K_o$ |
| $H_{vV}$ | 116 300 | J mol$^{-1}$ | Activation energy for $V_{c,\max}$ |
| $H_{dV}$ | 202 900 | J mol$^{-1}$ | Deactivation energy for $V_{c,\max}$ |
| $H_{vJ}$ | 79 500 | J mol$^{-1}$ | Activation energy for $J_{\max}$ |
| $H_{dJ}$ | 201 000 | J mol$^{-1}$ | Deactivation energy for $J_{\max}$ |
| $J_{\max 0}$ | 75 | $\mu$mol electrons m$^{-2}$ s$^{-1}$ | Eq. (B3) |
| $K_{c0}$ | 302 | $\mu$mol mol$^{-1}$ | Michaelis constant for $CO_2$ at $T_0$ |
| $K_{o0}$ | 256 | mmol mol$^{-1}$ | Michaelis constant for $O_2$ at $T_0$ |
| $o_i$ | 0.209 | mol mol$^{-1}$ | Oxygen concentration |
| $R$ | 8.31 | J mol$^{-1}$ K$^{-1}$ | Gas constant |
| $S_v$ | 650 | J mol$^{-1}$ | Entropy term |
| $T_0$ | 293.2 | K | Reference temperature |
| $V_{c,\max 0}$ | 50 | $\mu$mol m$^{-2}$ s$^{-1}$ | Eq. (B5) |
| $\beta_1$ | 0.9 | | Eq. (B4) |
| $\beta_2$ | 0.9 | | Eq. (B4) |
| $\gamma_0$ | 34.6 | $\mu$mol mol$^{-1}$ | $CO_2$ compensation point at $T_0$ |
| $\gamma_1$ | 0.0451 | K$^{-1}$ | Eq. (B5) |
| $\gamma_2$ | 0.000347 | K$^{-2}$ | Eq. (B5) |

by the model of Farquhar et al. (1980) for $C_3$ plants (e.g., Collatz et al. 1991; Leuning 1995; Foley et al. 1996). The model was originally proposed for $C_3$ plants but may be easily extended to $C_4$ plants (Collatz et al. 1992; Foley et al. 1996). Accordingly (see appendix B for details), when the leaf water potential is not limiting, the rate of $CO_2$ fixation is expressed as a function of three potential capacities to fix carbon, that is,

$$A_{\phi,c_i,T_l} = f(A_c, A_q, A_s), \tag{14}$$

where $A_c$ is the assimilation rate limited by rubisco activity (i.e., limited by $CO_2$ concentration), which depends on $c_i$, $T_l$, and atmospheric oxygen concentration, $o_i$; $A_q$ is the assimilation rate when the photosynthetic electron transport limits RuPB regeneration (light limitation), which depends on $\phi$, $c_i$, and $T_l$; and $A_s$ is the assimilation rate in conditions of high $c_i$ and $\phi$, when photosynthesis is limited only by $T_l$.

Equations (10) and (14) allow us to directly evaluate assimilation with Jarvis's approach after the other environmental variables are determined or to compute stomatal conductance, assimilation, and transpiration with Leuning's approach, when coupled to Eq. (9).

The stomatal function for Leuning's approach is thus

$$g_s = 1.6a_1 A_{\psi_l} A_{\phi,c_i,T_l}(\phi, c_i, T_l)\frac{f_D(D)}{c_s - \Gamma^*}, \tag{15}$$

which now has many similarities with Jarvis's Eq. (6). As shown by Fig. 1, the behavior of Eqs. (15) and (6) as a function of $D$, $\phi$, and $\psi_l$ is quite similar. However, an important difference between the two approaches is in the dependence of $g_s$ on $CO_2$ concentration. Jarvis's formula does not usually include a $CO_2$ control, consistent with the observation that stomata tend to remain open for very low $CO_2$ concentrations to favor assimilation, unless the other factors (i.e., $\phi$, $T_a$, $\psi_l$, and $D$) become limiting. In Eq. (15), instead, a double dependence on $CO_2$ concentration is present: one inherent in $A_n$ and the other in the corrective term $c_s - \Gamma^*$ introduced by Leuning (1995; see also Jarvis et al. 1999) to account for the fact that, when external $CO_2$ decreases toward the compensation point, the stomata tend to open, the other external parameters remaining the same. In this way, when $c_s$ tends to $\Gamma^*$, both net assimilation and $c_s - \Gamma^*$ tend to zero, leading to a finite (and higher than the usual values) limit for $g_s$.

## 5. Hourly dynamics

The system of equations (1), (2), (3), and (5) coupled to the stomatal function, Eqs. (6) or (9), and to the convective boundary layer model (appendix A) is solved numerically using the parameters given in Tables 1, 2, and 3 (unless otherwise specified) as well as the suitable initial conditions of soil moisture and boundary layer height. Assimilation is given by Eq. (12). The plant parameters are typical of a $C_3$ woody plant adapted to semiarid conditions (e.g., Scholes and Walker 1993).

Figure 3 shows the temporal dynamics of some of the main variables characterizing the SPAC during a dry down of several days. It is apparent how soil moisture decays more slowly during the night for lack of transpiration. Leaf water potential is equal to soil water potential during the night, while during the day it is much lower because of transpiration (Fig. 3b). Through the energy balance, transpiration also influences the boundary layer, affecting leaf temperature (not shown) and the potential saturation deficit (Fig. 3c); $D$ and $\psi_l$ affect stomatal behavior and, in turn, cause a reduction in assimilation (Fig. 3f). Both the daily maximum assimilation and minimum leaf water potential decrease with time, while the maximum $D$ increases. The carbon concentration inside the stomata (not shown), driven by

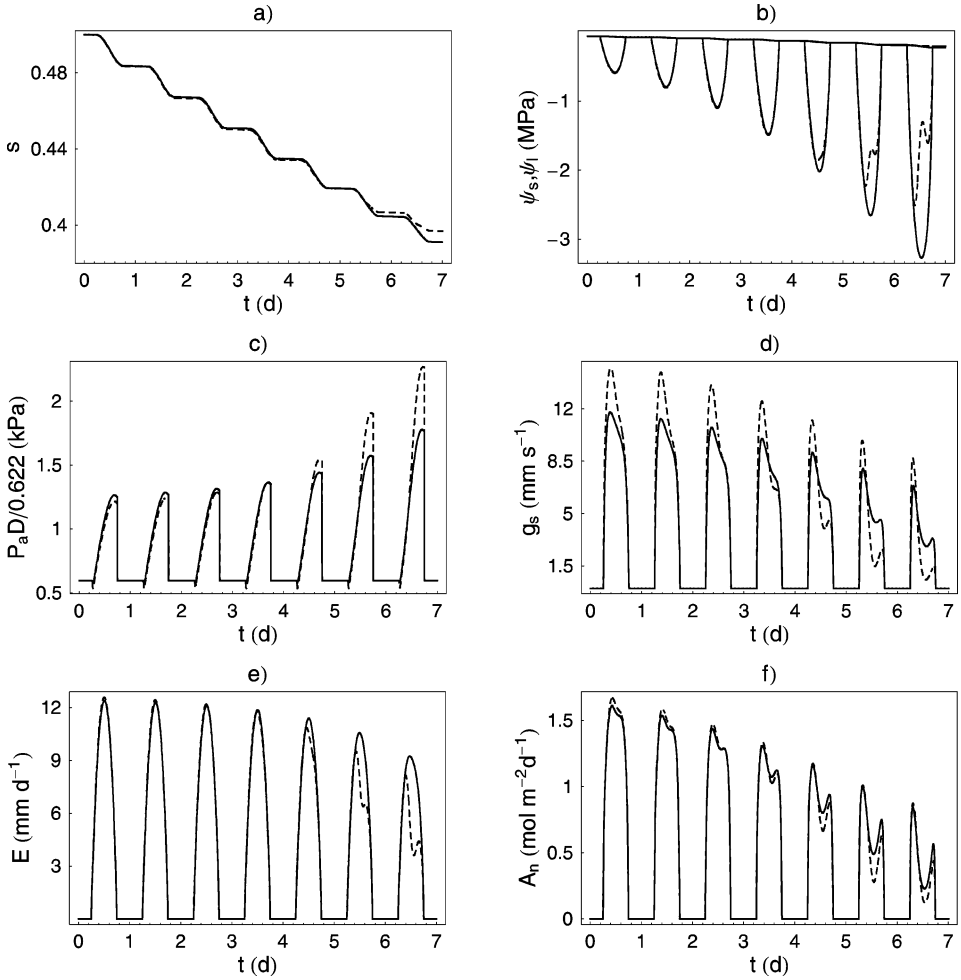


FIG. 3. Results at hourly time scale using Jarvis's approach (continuous line) and Leuning's formulation (dashed line), with an initial value of $s$ equal to 0.45; $R_{AI} = 5.6$, $L_{AI} = 1.4$, and $Z_r = 60$ cm; soil is a loam with parameters as in Table 2. Plant parameters as in Tables 1 and 3.

the assimilation rate, is lower during the day (at night $c_i$ is imposed equal to $c_a$).

Figure 3 also highlights some differences due to the two stomatal functions. The higher leaf water potential given by Leuning leads to higher assimilation even in the afternoon, in spite of the faster stomata closure (Fig. 3d). With Jarvis's formulation, the maximum transpiration and assimilation are higher, while the afternoon decay of $E$ and $A_n$ is slower, thereby giving a faster soil water depletion (see Fig. 3a). For both approaches stomatal conductance has a maximum in the morning, then reaches a plateau in the afternoon, and finally goes to zero at night, when stomata are closed (Figs. 4a,b). Stomata quickly open in the morning when radiation starts and then partially close for the effect of $D$ and $\psi_l$; the plateau in the afternoon is related to the reduction of $\phi$, and the increments in $D$ and $T_a$ are compensated by the positive effect of higher leaf water potentials. These behaviors are in agreement with the previous results in the literature (e.g., Collatz et al. 1991, and references therein). In well-watered conditions, both formulations give about the same transpiration (cf. Figs. 4c,d) and assimilation (cf. Figs. 4e,f) rates. When soil moisture decreases, instead, Leuning's formula leads to lower $E$ and $A_n$. With Jarvis's formulation the daily course of $E$ is rather symmetrical, while with Leuning's it more closely follows that of $g_s$, so that in the afternoon it tends to be lower.

The water use efficiency (WUE), defined as the ratio of $A_n/A_{max}$ over $E/E_{max}$, being $A_{max}$ and $E_{max}$ net assimilation and transpiration rate averaged over a day in well-watered conditions, also presents some differences with the two formulations (Figs. 5a,b). In both cases the WUE reaches its peak value in the early morning, when transpiration is hindered by the moister air, and assimilation is growing for the increasing solar irradiance. As the air humidity declines during the day so does WUE until the late afternoon, when the situation is reversed

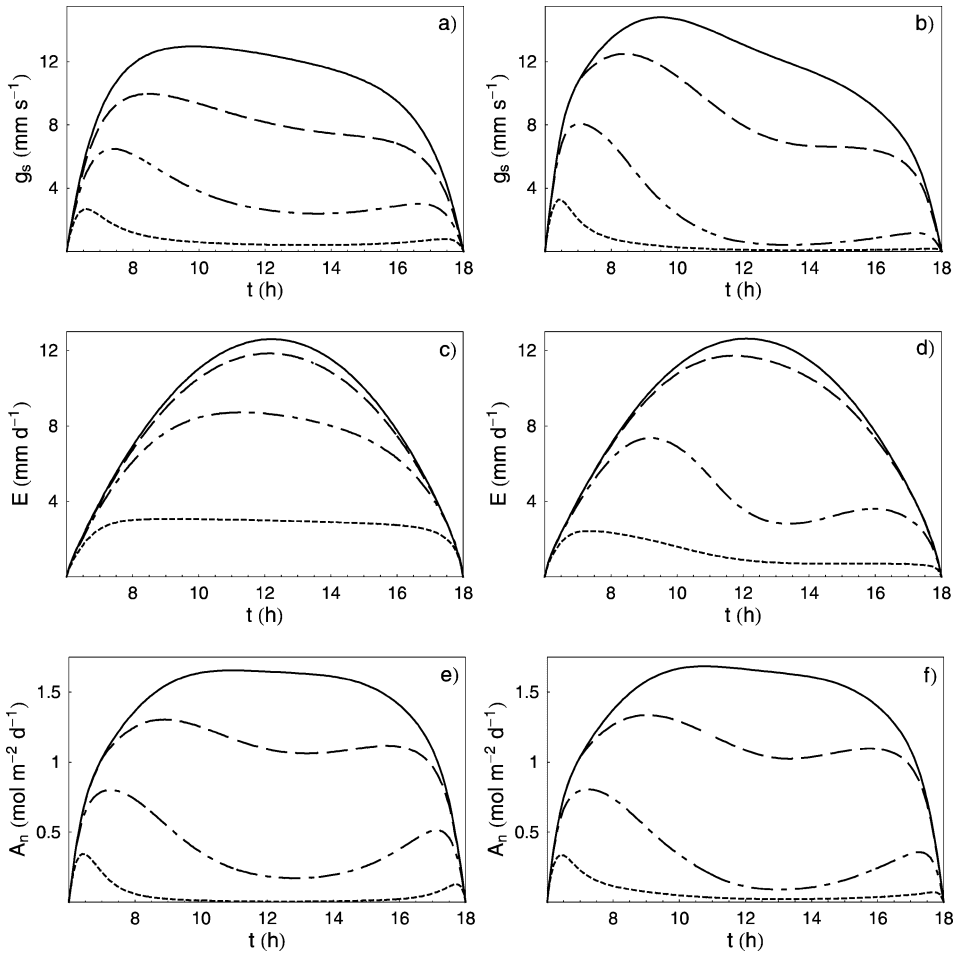


FIG. 4. Results at hourly time scale following (left) Jarvis's and (right) Leuning's formulation for different initial soil moisture levels: $s = 1$ (continuous line), 0.45 (dashed line), 0.4 (chain line), and 0.35 (dotted line). Parameters as in Fig. 3.

by the slower decay of assimilation compared to transpiration. The fact that the maximum is reached in the morning is probably due to the dominant increase of solar radiation compared to the reduction of water potential that follows stomatal opening.

Some differences between the two approaches in the evaluation of the water use efficiency are shown in Fig. 6. With Jarvis's formulation the early-morning high values of WUE tend to increase at the beginning of the dry down, but they dramatically decrease when soil moisture level becomes lower than a certain value (as will be seen in Part II, the value of $s$ at which WUE starts diminishing approximately corresponds to the soil moisture level $s^*$, below which a plant can be considered

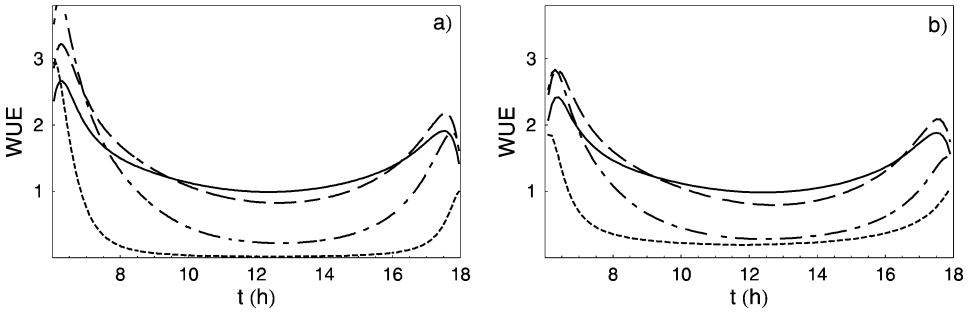


FIG. 5. Daily behavior of WUE following (a) Jarvis's and (b) Leuning's approach for different initial soil moisture levels, as in Fig. 4.

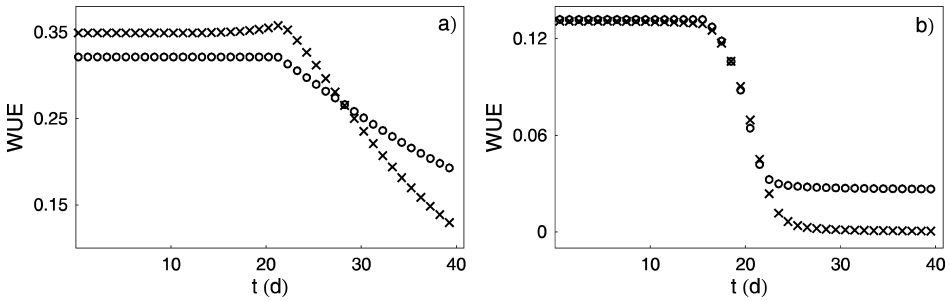


FIG. 6. (a) Early morning and (b) midday values of WUE as a function of time during soil dry down, following Jarvis (×) and Leuning (○); parameters as in Fig. 3.

under water stress conditions). A steeper drop is evident for the WUE evaluated at midday. A similar pattern also holds for Leuning's approach, which leads to lower early-morning values of WUE under well-watered conditions and gives higher WUE in conditions of low soil moisture. This difference is due to the dependence of stomatal conductance on net assimilation in Leuning's formulation, that, unlike Jarvis's, couples $A_n$ to $E$.

This last analysis of the results at the hourly time scale partly anticipates the results of the scaling at the daily time scale (see next section and Part II). In fact, it already shows the existence of two different regimes in the assimilation dynamics of the plant: an unstressed one, in which soil moisture deficit does not affect WUE, and a subsequent one of progressive worsening of plant water stress with decreasing WUE.

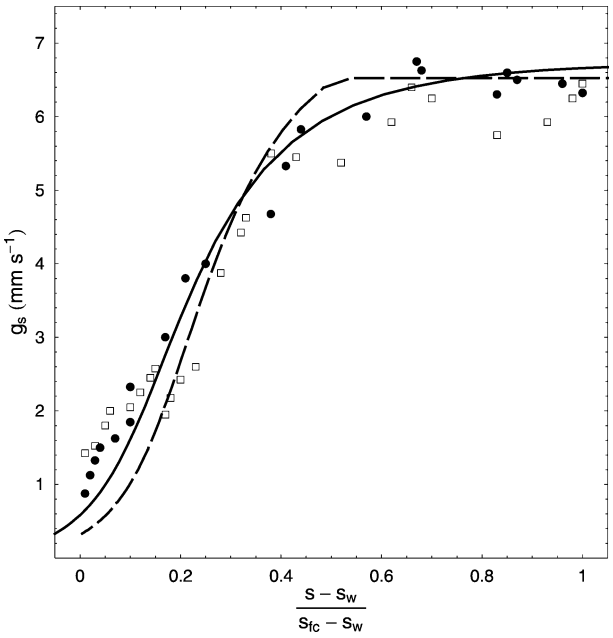


FIG. 7. Stomatal conductance $g_s$ as a function of the extractable soil moisture for *Nerium oleander* measured maintaining constant irradiance and two different levels of vapor pressure deficit [solid circles and open squares; after Gollan et al. (1985)]. Comparison with model results of stomatal conductance sampled every day at a given time for Jarvis's (continuous line) and Leuning's (dashed line) formulation. The time of the sampling is chosen so as to ensure the same stomatal conductances as the measured data under well-watered conditions. The extractable soil moisture is defined using typical values for loamy soil and $C_3$ plants of the wilting point, $s_w = 0.20$, and the field capacity, $s_{fc} = 0.55$.

## 6. Comparison with data

A close inspection of the diurnal patterns of transpiration and assimilation (Figs. 3 and 4) actually shows that they are modulated mostly by the changes in soil water potential. The trends of their mean values are thus expected to be more regular, allowing simple and parsimonious modeling of daily transpiration, assimilation, and soil moisture dynamics. Examples and detailed discussion of the upscaling at the daily level will be given in Part II. Here we only analyze and compare with measured data the functional dependence of leaf conductance on relative soil moisture at the daily level. Figure 7 compares the model results with the measured leaf conductance of the $C_3$ plant *Nerium oleander* (Gollan et al. 1985) as a function of the so-called extractable soil moisture. As the measurements were conducted under constant irradiance, the model results during a phase of dry down are sampled at a given hour of the day to ensure constant irradiance. The time of the sampling is chosen so that the modeled stomatal conductance matched the measurements at high soil water contents. The general behavior is very well reproduced for both approaches, with a plateau for well-watered conditions and a regular (almost linear) decay at low soil moisture values. As will be seen in Part II, a similar trend will be shown to hold also for transpiration [in agreement with previous results in the literature (e.g., Federer 1979)] and assimilation.

## 7. Conclusions

A relatively simple model of soil water balance, transpiration, and photosynthesis, valid at the hourly time scale, has been developed and analyzed, linking the water flow from the soil to the atmosphere to the soil and plant characteristics and comparing the two empirical approaches of Jarvis and Leuning of stomatal functioning.

The results during a progressive soil moisture depletion show that the diurnal trends of transpiration, plant water potential, and leaf carbon assimilation by photosynthesis are realistically captured going from well-watered to advanced-drought conditions (Slatyer 1967; Larcher 1995). In spite of their differences, the two approaches for stomatal functioning have given similar diurnal trends of transpiration and assimilation (as will be seen in Part II, this similarity is even more evident for daily transpiration and assimilation rates), thus providing confidence in the temporal upscaling. The results of this paper are employed in Part II to analyze the daily time scale dynamics of assimilation and to investigate the role of soil and plant characteristics on transpiration, photosynthesis, and soil moisture dynamics under fluctuating climatic conditions.

*Acknowledgments.* We are grateful to John Albertson and Andrew Guswa for their useful comments. We acknowledge the support of the National Science Foundation through grants Biocomplexity (DEB-0083566) and National Center for Earth Surface Dynamics (EAR-0120914).

## APPENDIX A

### Transpiration and Convective Boundary Layer Modeling

The time course of specific humidity $q$ and potential temperature $\vartheta$ of the atmosphere are obtained by modeling the boundary layer growth according to the scheme of McNaughton and Spriggs (1986) and Lhomme et al. (1998). Representing the convective boundary layer as a well-mixed slab of air of thickness $h$ with constant profiles of $q$ and $\vartheta$, the equations for heat and water balance are

$$\rho c_p h \frac{d\vartheta}{dt} = H + \rho c_p(\vartheta_s - \vartheta)\frac{dh}{dt},$$

$$\rho h \frac{dq}{dt} = \rho_w E + \rho(q_s - q)\frac{dh}{dt}, \qquad \text{(A1)}$$

where $\vartheta_s$ and $q_s$ are the potential temperature and the humidity at height $h$, respectively, and $H$ is the sensible heat flux from vegetation, $\phi - \lambda_w \rho_w E$. The effect of the sensible and latent heat fluxes from the soil are assumed to be negligible compared to those from vegetation. The boundary layer growth rate is expressed as

$$\frac{dh}{dt} = \frac{H}{\rho c_p h \gamma_\vartheta}, \qquad \text{(A2)}$$

with $\gamma_\vartheta$ the gradient of the potential temperature at height $h$. The temperature and humidity profiles in the overlying undisturbed atmosphere are assumed to be linear (Lhomme et al. 1998),

$$\vartheta_s = \gamma_\vartheta z + \vartheta_{s0} = 4.78z + 293.6,$$

$$q_s = \gamma_q z + q_{s0} = -0.002\,85z + 0.011\,66, \qquad \text{(A3)}$$

with $z$ (evaluated at $z = h$) in kilometers, $\vartheta$ in kelvin, and $q$ in kilograms per kilogram. For simplicity, the leaf available energy, $\phi(t)$, is assumed to be independent of leaf area index and equal to the effective solar radiation reaching the leaves. This is modeled as $\phi(t) = (4\phi_{\max}/\delta^2)[-t^2 + (\delta + 2t_0)t - t_0(t_0 + \delta)]$, with maximum available energy $\phi_{\max} = 500$ W m$^{-2}$, day length $\delta = 12$ h, and $t_0 = 6$ h (e.g., Lhomme et al. 1998).

## APPENDIX B

### Assimilation Model for $C_3$ Plant

Assimilation in Eq. (14) is modeled following Farquhar et al. (1980) and the corrections by Collatz et al. (1991), Leuning (1995), and Foley et al. (1996). The Rubisco-limited rate of photosynthesis is given by

$$A_c = V_{c,\max}\frac{c_i - \Gamma^*}{c_i + K_c(1 + o_i/K_o)}, \qquad \text{(B1)}$$

where $V_{c,\max}$ is the maximum carboxylation rate; $K_c$ and $K_o$ are the Michaelis–Menten coefficients for $CO_2$ and $O_2$, respectively; and $\Gamma^*$ is the $CO_2$ compensation point. These are given below, while the oxygen concentration, $o_i$, is assumed to be constant (Collatz et al. 1991). The assimilation rate when the photosynthetic electron transport limits RuPB regeneration (light limitation) is

$$A_q = \frac{J}{4}\frac{c_i - \Gamma^*}{(c_i + 2\Gamma^*)}, \qquad \text{(B2)}$$

where $J$ is the electron transport rate when the absorbed photon irradiance is $Q$ (expressed in mol photons m$^{-2}$ s$^{-1}$ and assumed to be proportional to the leaf available energy) and is given by the lower root of the equation, $\kappa_1 J^2 - (\kappa_2 Q + J_{\max})J + \kappa_2 Q J_{\max} = 0$, where $\kappa_1 = 0.95$, $\kappa_2 = 0.20$ mol electrons mol$^{-1}$ photons (Leuning 1995), $J_{\max}$ is

$$J_{\max} = J_{\max 0}\frac{\exp\left[\dfrac{H_{vJ}}{\mathrm{R}T_0}\left(1 - \dfrac{T_0}{T_l}\right)\right]}{1 + \exp\left(\dfrac{S_v T_l - H_{dJ}}{\mathrm{R}T_l}\right)}, \qquad \text{(B3)}$$

with the parameters as in Table 3, and $A_s$ is approximately the maximum value of net assimilation in saturating conditions of carbon concentration and irradiance, modeled as (Collatz et al. 1991), $A_s = V_{c,\max}/2$.

To account for the gradual transition among the three carbon assimilation rates and obtain $A_{\phi,c_i,T_l}$ in Eq. (14), Collatz et al. (1991) proposed to use the roots of the following set of equations

$$\beta_1 A_p^2 - (A_c + A_q)A_p + A_c A_q = 0$$

$$\beta_2 A_{\phi,c_i,T_l}^2 - (A_p + A_s)A_{\phi,c_i,T_l} + A_p A_s = 0, \qquad \text{(B4)}$$

where $A_p$ is an intermediate value that gives the minimum between $A_c$ and $A_q$, and $\beta_1$ and $\beta_2$ are empirical constants (see Table 3). The Michaelis–Menten coefficients, the maximum carboxylation rate, and the $T_l$ dependence of the $CO_2$ carboxylation point are modeled using the following empirical functions (Leuning 1995):

$$K_x = K_{x0} \exp\left[\frac{H_x}{\mathrm{RT}_0}\left(1 - \frac{T_0}{T_l}\right)\right],$$

$$\Gamma^* = \gamma_0[1 + \gamma_1(T_l - T_0) + \gamma_2(T_l - T_0)^2],$$

$$V_{c,\max} = V_{c,\max 0}\frac{\exp\left[\dfrac{H_{vV}}{\mathrm{RT}_0}\left(1 - \dfrac{T_0}{T_l}\right)\right]}{1 + \exp\left(\dfrac{S_v T_l - H_{dV}}{\mathrm{RT}_i}\right)}, \quad \text{(B5)}$$

where $x$ stands for $c$ or $o$, and the terms are reported in Table 3.

## REFERENCES


Baldocchi, D., and T. Meyers, 1998: On using eco-physiological, micrometeorological and biogeochemical theory to evaluate carbon dioxide, water vapor and trace gas fluxes over vegetation: A perspective. *Agric. For. Meteor.,* **90,** 1–25.

Ball, J. T., I. E. Woodrow, and J. A. Berry, 1987: A model predicting stomatal conductance and its contribution to the control of photosynthesis under different environmental conditions. *Progress in Photosynthesis Research,* J. Biggens, Ed., Vol. IV, Martinus Nijhoff, 221–224.

Bonan, G. B., 1995: Land–atmosphere $CO_2$ exchange simulated by a land surface process model coupled to an atmospheric general circulation model. *J. Geophys. Res.,* **100,** 2817–2831.

——, 2002: *Ecological Climatology: Concepts and Applications.* Cambridge University Press, 678 pp.

Brubaker, K. L., and D. Entekhabi, 1995: An analytic approach to modeling land–atmosphere interaction. 1. Construct and equilibrium behavior. *Water Resour. Res.,* **31,** 619–632.

Campbell, G. S., and J. M. Norman, 1998: *An Introduction to Environmental Biophysics.* Springer, 286 pp.

Clapp, R. B., and G. N. Hornberger, 1978: Empirical equations for some soil hydraulic properties. *Water Resour. Res.,* **14,** 601–604.

Collatz, J. G., J. T. Ball, C. Grivet, and J. A. Berry, 1991: Physiological and environmental regulation of stomatal conductance, photosynthesis and transpiration: A model that includes a laminar boundary layer. *Agric. For. Meteor.,* **54,** 107–136.

——, M. Ribas-Carbo, and J. A. Berry, 1992: Coupled photosynthesis-stomatal conductance model for leaves of $C_4$ plants. *Aust. J. Plant Physiol.,* **19,** 519–538.

Cordoba, J. R., and R. L. Bras, 1981: Physically based probabilistic models of infiltration, soil moisture, and actual evapotranspiration. *Water Resour. Res.,* **17,** 93–106.

Daly, E., A. Porporato, and I. Rodriguez-Iturbe, 2004: Coupled dynamics of photosynthesis, transpiration, and soil water balance. Part II: Stochastic analysis and ecohydrological significance. *J. Hydrometeor.,* **5,** 559–566.

Dewar, R. C., 1995: Interpretation of an empirical model for stomatal conductance in terms of guard cell function. *Plant Cell Environ.,* **18,** 365–372.

Dickinson, R. E., A. Henderson-Sellers, P. J. Kennedy, and M. F. Wilson, 1986: Biosphere–Atmosphere Transfer Scheme (BATS) for the NCAR CCM. Tech. Note NCAR/TN-275-STR, National Center for Atmosphere Research, Boulder, CO.

——, and Coauthors, 2002: Nitrogen control on climate model evapotranspiration. *J. Climate,* **15,** 278–295.

Dingman, S. L., 1994: *Physical Hydrology.* Prentice Hall, 575 pp.

D'Odorico, P., F. Laio, A. Porporato, and I. Rodriguez-Iturbe, 2003: Hydrologic controls on soil carbon and nitrogen cycles. II. A case study. *Adv. Water Res.,* **26,** 59–70.

Elthair, E. A. B., 1998: A soil moisture-rainfall mechanism. 1. Theory and observations. *Water Resour. Res.,* **34,** 765–776.

Farquhar, G. D., S. von Cammerer, and J. A. Berry, 1980: A biochemical model of photosynthetic $CO_2$ assimilation in leaves of $C_3$ species. *Planta,* **149,** 78–90.

Federer, C. A., 1979: A soil–plant–atmosphere model for transpiration and availability of soil water. *Water Resour. Res.,* **15,** 555–561.

Foley, A. J., I. Colin Prentice, N. Ramankutty, S. Levis, D. Pollard, S. Sitch, and A. Haxeltine, 1996: An integrated biosphere model of land surface processes, terrestrial carbon balance and vegetation dynamics. *Global Biogeochem. Cycles,* **10,** 603–628.

Gollan, T., N. C. Turner, and D. Schulze, 1985: The responses of stomata and leaf gas exchange to vapour pressure deficit and soil water content. III. In the schlerophyllous woody species *Nerium oleander*. *Oecologia,* **65,** 356–362.

Guswa, A. J., M. A. Celia, and I. Rodriguez-Iturbe, 2002: Models of soil moisture dynamics in ecohydrology: A comparative study. *Water Resour. Res.,* **38,** 1166, doi:10.1029/2001WR000826.

Jarvis, A. G., T. A. Mansfield, and W. J. Davies, 1999: Stomatal behavior, photosynthesis and transpiration under rising $CO_2$. *Plant Cell Environ.,* **22,** 639–648.

Jarvis, P. G., 1976: The interpretation of the variations in leaf water potential and stomatal conductance found in canopies in the field. *Philos. Trans. Roy. Soc. London,* **B273,** 593–610.

——, and K. G. McNaughton, 1986: Stomatal control of transpiration: Scaling up from leaf to region. *Adv. Ecol. Res.,* **15,** 1–49.

Jones, H. G., 1992: *Plant and Microclimate: A Quantitative Approach to Environmental Plant Physiology.* Cambridge University Press, 428 pp.

Katul, G., R. Leuning, and R. Oren, 2003: Relationship between plant hydraulic and biochemical properties derived from a steady state coupled water and carbon transport model. *Plant Cell Environ.,* **26,** 339–350.

Knapp, A. K., and Coauthors, 2002: Rainfall variability, carbon cycling, and plant species diversity in a mesic grassland. *Science,* **298,** 2202–2205.

Laio, F., A. Porporato, L. Ridolfi, and I. Rodriguez-Iturbe, 2001: Plants in water-controlled ecosystems: Active role in hydrologic processes and response to water stress. II. Probabilistic soil moisture dynamics. *Adv. Water Res.,* **24,** 707–723.

Larcher, W., 1995: *Physiological Plant Ecology.* 3d ed. Springer, 509 pp.

Leuning, R., 1990: Modeling stomatal behavior and photosynthesis of *Eucalyptus grandis*. *Aust. J. Plant Physiol.,* **17,** 159–175.

——,1995: A critical appraisal of a combined stomatal-photosynthesis model for $C_3$ plants. *Plant Cell Environ.,* **18,** 339–355.

——, F. M. Kelliher, D. G. G. De Pury, and E. D. Schulze, 1995: Leaf nitrogen, photosynthesis, conductance and transpiration: Scaling from leaves to canopies. *Plant Cell Environ.,* **18,** 1183–1200.

Lhomme, J. P., 2001: Stomatal control of transpiration: Examination of the Jarvis-type representation of canopy resistance in relation to humidity. *Water Resour. Res.,* **37,** 689–699.

——, E. Elguero, A. Chehbouni, and G. Boulet, 1998: Stomatal control of transpiration: Examination of Monteith's formulation of canopy resistance. *Water Resour. Res.,* **34,** 2301–2308.

Lohammer, T., S. Larsson, S. Linder, and S. O. Falk, 1980: FAST—Simulation models of gaseous exchange in Scots Pine. *Ecol. Bull.,* **32,** 505–523.

McNaughton, K. G., and T. W. Spriggs, 1986: A mixed layer model for regional evaporation. *Bound.-Layer Meteor.,* **34,** 243–262.

Nobel, P. S., 1999: *Physicochemical and Environmental Plant Physiology.* 2d ed. Academic Press, 474 pp.

Noy-Meir, I., 1973: Desert ecosystems: Environment and producers. *Annu. Rev. Ecol. Syst.,* **4,** 25–51.

Pollard, D., and S. L. Thompson, 1995: Use of a land-surface-transfer scheme (LSX) in a global climate model (GENESIS): The response to doubling stomatal resistance. *Global Planet. Change,* **10,** 129–161.

Porporato, A., and I. Rodriguez-Iturbe, 2002: Ecohydrology—A challenging multidisciplinary research perspective. *J. Hydrol. Sci.,* **47,** 811–821.

——, P. D'Odorico, L. Ridolfi, and I. Rodriguez-Iturbe, 2000: A spatial model for soil–atmosphere interaction: Model construction and linear stability analysis. *J. Hydrometeor.,* **1,** 61–74.

——, F. Laio, L. Ridolfi, and I. Rodriguez-Iturbe, 2001: Plants in water-controlled ecosystems: Active role in hydrologic processes and response to water stress. III. Vegetation water stress. *Adv. Water Res.,* **24,** 725–744.

——, P. D'Odorico, F. Laio, and I. Rodriguez-Iturbe, 2003: Hydrologic controls on soil carbon and nitrogen cycles. I. Modeling scheme. *Adv. Water Res.,* **26,** 45–58.

Rodriguez-Iturbe, I., A. Porporato, L. Ridolfi, V. Isham, and D. R. Cox, 1999: Probabilistic modeling of water balance at a point: The role of climate, soil and vegetation. *Proc. Roy. Soc. London,* **A455,** 3789–3805.

Scholes, R. J., and B. H. Walker, 1993: *An African Savanna.* Cambridge University Press, 306 pp.

Sellers, P. J., Y. Mintz, Y. C. Sud, and A. Dalcher, 1986: A Simple Biosphere model (SiB) for use within general circulations models. *J. Atmos. Sci.,* **43,** 505–531.

——, and Coauthors, 1997: Modeling the exchanges of energy, water, and carbon between continents and the atmosphere. *Science,* **275,** 502–509.

Siqueira, M., G. Katul, and C.-T. Lai, 2002: Quantifying net ecosystem exchange by multilevel ecophysiological and turbulent transport models. *Adv. Water Resour.,* **25,** 1357–1366.

Slatyer, R. O., 1967: *Plant–Water Relationships.* Academic Press, 366 pp.

Sperry, J. S., F. R. Adler, G. S. Campbell, and J. P. Comstock, 1998: Limitation of plant water use by rhizosphere and xylem conductance: Results from a model. *Plant Cell Environ.,* **21,** 347–359.

——, U. G. Hacke, R. Oren, and J. P. Comstock, 2002: Water deficits and hydraulic limits to leaf water supply. *Plant Cell Environ.,* **25,** 251–263.

Stephenson, N. L., 1990: Climatic control of vegetation distribution: The role of the water balance. *Amer. Nat.,* **135,** 649–670.

Tezara, W., V. J. Mitchell, S. D. Driscoll, and D. W. Lawlor, 1999: Water stress inhibits plant photosynthesis by decreasing coupling factor and ATP. *Nature,* **401,** 914–917.

van den Honert, T. H., 1948: Water transport as a catenary process. *Discuss. Faraday Soc.,* **3,** 146–153.

Williams, M., and Coauthors, 1996: Modelling the soil–plant–atmosphere continuum in a Quercus-Acer stand at Harvard forest: The regulation of stomatal conductance by light, nitrogen and soil/plant hydraulic properties. *Plant Cell Environ.,* **19,** 911–927.